Supporting Information

Comparison of Energy Efficiency and Power Density in Pressure Retarded Osmosis and Reverse Electrodialysis

Ngai Yin Yip and Menachem Elimelech*

Department of Chemical and Environmental Engineering
Yale University
New Haven, CT 06520-8286, USA

* Corresponding author: Email: menachem.elimelech@yale.edu

Driving Force Approximations Using Molar Concentration. The osmotic pressure difference, $\Delta\pi$, across an ideal semipermeable membrane (i.e., rejects salt perfectly) separating a high concentration (HC) and a low concentration (LC) solution is[1]

$$\Delta\pi = \frac{R_g T}{\overline{V}} \ln\left(\frac{\gamma_{w,LC} x_{w,LC}}{\gamma_{w,HC} x_{w,HC}}\right) \quad \text{(S1)}$$

where R_g is the gas constant, T is the absolute temperature, and $\overline{V}$ is the water molar volume. The activity coefficient and mole fraction of water is denoted by γ_w and x_w, respectively. For relatively low salinities, γ_w is ~1 (Figure S1).[1, 2] Because $x_w = 1 - \nu x_s$, the mole fraction of water can be approximated with $1 - \nu c\overline{V}$ (c is the molar concentration while ν is the number of aqueous species each solute contributes to the electrolyte solution, i.e., ν = 2 for NaCl). Thus, molar concentration of the solutions can be used in the van't Hoff equation to estimate $\Delta\pi$:

$$\Delta\pi \approx \nu R_g T\left(c_{HC} - c_{LC}\right) \quad \text{(S2)}$$

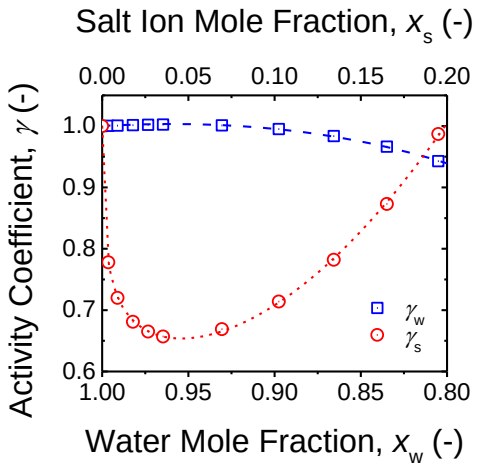

Figure S1. Water and salt activity coefficients (blue square and red circle symbols, respectively) as a function of the mole fraction of water for an NaCl electrolyte solution, using activity coefficient, osmotic coefficient, molal concentration (moles of solute per unit mass of solvent), and solution density data from literature.[2] The blue dashed and red dotted lines denote the fitting equations, eqs S3 and S4, respectively:

$$\gamma_w = -1.9407\left(\ln x_w\right)^2 - 0.1605 \ln x_w + 1 \qquad R^2 = 0.9986 \quad \text{(S3)}$$

$$\gamma_s = -0.06602 \ln\left(x_s - 0.0001217\right) + 9.563 x_s^{\,2} + 0.5551 x_s + 0.4049 \qquad R^2 = 0.9997 \quad \text{(S4)}$$

However, at high salt concentrations (i.e., x_w is substantially smaller than one), γ_w deviates significantly from unity (Figure S1) and $1-\nu c\bar{V}$ is also less accurate in estimating x_w. Therefore, the simplifying van't Hoff equation, eq S2, is anticipated to depart from eq S1. Osmotic pressure difference calculated using $\gamma_w x_w$ and c (solid and dashed blue lines, respectively) as a function of HC solution (NaCl) concentration are presented in Figure S2 (left vertical axis). The LC solution is 1.5 mM NaCl while the temperature is 298 K. At c_{HC} = 4 M NaCl, the discrepancy between $\Delta\pi$ calculated using eqs S1 and S2 is largest (~20%).

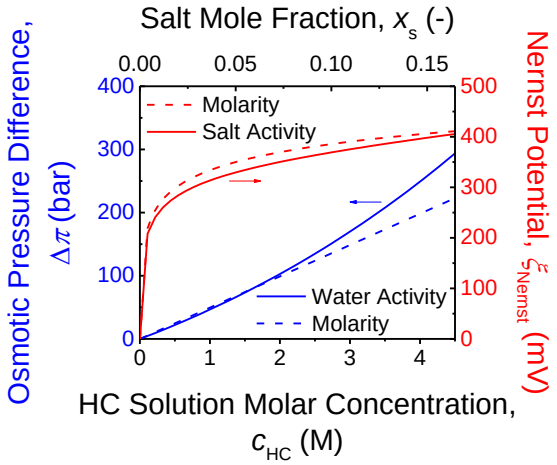

Figure S2. Osmotic pressure difference, $\Delta\pi$ (blue lines, left vertical axis), and Nernst potential, ξ_{Nernst} (red lines, right vertical axis), between a HC (NaCl) solution and a 1.5 mM NaCl LC solution, as a function of the HC solution molar concentration, c_{HC}. Solid lines indicate the driving force calculated using activity coefficients and mole fractions (eqs S1 and S5), while dashed lines denote $\Delta\pi$ and ξ_{Nernst} determined with the simplified relations (eqs S2 and S6). The salt-rejecting membranes and ion exchange membranes are assumed to be perfectly selective, and the temperature T is 298K.

Similarly, the Nernst potential, ξ_{Nernst}, across a pair of perfectly selective cation and anion exchange membranes separating two solutions of different concentration can be determined using the activity coefficient, γ_s, and mole fraction, x_s, of the salt (as Na^+ and Cl^- ions):[3]

$$\xi_{Nernst} = \frac{2R_gT}{zF}\ln\left(\frac{\gamma_{s,HC}x_{s,HC}}{\gamma_{s,LC}x_{s,LC}}\right) \tag{S5}$$

where z is the ion valence (i.e., 1 for NaCl), F is the Faraday constant, and the factor of 2 accounts for the ion exchange membrane pair. Although γ_s deviates from unity even at relatively

small concentrations (Figure S1), natural logarithm of the salt activity, $\ln(\gamma_s x_s)$, is dominated by the mole fraction term.[1, 2] Therefore, the ratio of the HC and LC solution mole fraction can be taken to be the molar concentration ratio for relatively low salinities. The Nernst equation, hence, simplifies to

$$\xi_{\text{Nernst}} \approx \frac{2R_g T}{zF} \ln\left(\frac{c_{\text{HC}}}{c_{\text{LC}}}\right) \tag{S6}$$

The Nernst potentials calculated using eqs S5 and S6, as a function of c_{HC}, are shown in Figure S2 (right vertical axis, solid and dashed red lines, respectively). Temperature and c_{LC} are the same as $\Delta\pi$ plot. Compared to osmotic pressure difference, the simplification for ξ_{Nernst} yields less deviation (<7%), with the greatest different occurring at ~0.6 M NaCl (salinity of seawater).

Practical Operation of PRO and RED. As controlled mixing progresses, the concentration of the HC solution nears that of the LC solution in RED, while the osmotic pressure difference approaches the applied hydraulic pressure in PRO. Hence, the driving force for water and ion flux is gradually diminished. Because of the reduced permeation rate, the power density is unfavorably lowered towards the end of the process. In other words, converting the last bit of salinity energy to useful work will be innately slow. Although carrying out PRO and RED to completion can extract the most energy, the resultant power density will also be considerably reduced. Our recent study indicates that judicious early discontinuation of RED yields significantly enhanced power density, PD, with only marginal forfeit in efficiency, η.[4] To model practical operation, triggers for early process termination were rationally selected in this study (after 90% and 70% of the eventual water and ion permeation for PRO and RED, respectively) to achieve power density improvements with reasonably minor efficiency losses.

Figure S3 shows a representative plot of PD and η for a range of constant applied hydraulic pressure, ΔP, in PRO (blue square symbols) and constant external load resistance, R_{L}, in RED (red circle symbols). In this illustrative analysis, natural salinity gradient (i.e., 600 mM–1.5 mM NaCl) was used with PRO-I and RED-I membranes (properties listed in Table 1 of the main manuscript). As ΔP is raised from 0 to 29.7 bar in PRO (blue directional arrows), both PD and η increase from zero until maximum power density is attained (2.9 W/m^2). Further raising ΔP

lowers PD but continues to improve the efficiency to its peak value (53.9%), beyond which both PD and η diminish with increasing ΔP. RED exhibits a different trend when increasingly larger R_L is employed (red directional arrows): PD initially rises to achieve maximum power density (0.77 W/m^2) and subsequently decreases back to zero at infinitely high R_L, while efficiency increases monotonically from 0 to ~83.1%. Note that the applied hydraulic pressure in PRO is capped by the osmotic pressure difference between the HC and LC solutions (29.7 bar in this scenario), whereas there is no operating constraint in RED to limit the external load resistance that can be utilized.

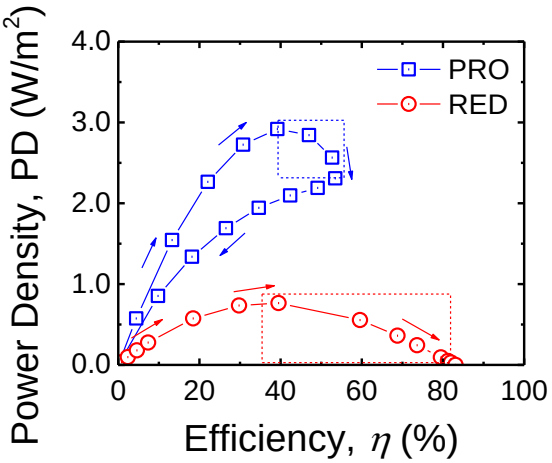

Figure S3. Representative plot of power density, PD, and efficiency, η, for a range of constant applied hydraulic pressure, ΔP, in PRO (blue square symbols) and constant external load resistance, R_L, in RED (red circle symbols). Dotted boxes specify the practical operating region, as points outside have either lower PD or η, or simultaneously both reduced PD and η. Natural salinity gradient (i.e., 600 mM–1.5 mM NaCl) was employed for this illustration, and the membranes used in the analysis are PRO-I and RED-I (properties listed in Table 1 of the main manuscript). Directional arrows indicate increasing ΔP (0–29.7 bar) and $R_L A_m$ (0–∞ Ωcm^2), with A_m being the effective membrane area of the RED stack.

The combinations of PD and η within the dotted boxes in Figure S3 are always higher than points outside. Thus, the range of ΔP and R_L demarcated by the boxes signify the practical operating regions for PRO and RED. The slope of the PD-η curves is negative in these operating regions, indicating a tradeoff between the two performance parameters: an increase in power density is always accompanied by a decrease in energy efficiency, and vice versa. Comparing the two operating regions reveals that RED with constant external load resistance allows much

higher efficiencies to be achieved (up to 83% compared to 54% for PRO). However, the large R_L necessary to attain very high η will result in impractically low PD. The comparisons presented in this study will, thus, focus solely on RED performance when PD is maximized. On the other hand, peak η can be obtained in constant-pressure PRO with a non-zero PD. The analyses will present PRO performance when η is maximized.

REFERENCES

1. Robinson, R. A.; Stokes, R. H., *Electrolyte solutions*. 2nd rev. ed.; Dover Publications: Mineola, NY, **2002**; p xv, 571 p.

2. Pitzer, K. S.; Peiper, J. C.; Busey, R. H., Thermodynamic Properties of Aqueous Sodium Chloride Solutions. *Journal of Physical and Chemical Reference Data* **1984,** *13*, (1), 1-102.

3. Weinstein, J. N.; Leitz, F. B., Electric-Power from Difference in Salinity - Dialytic Battery. *Science* **1976,** *191*, (4227), 557-559.

4. Yip, N. Y.; Vermaas, D. A.; Nijmeijer, K.; Elimelech, M., Thermodynamic, Energy Efficiency, and Power Density Analysis of Reverse Electrodialysis Power Generation with Natural Salinity Gradients. *Environ Sci Technol* **2014,** *48*, (9), 4925-4936.

Table S1. The Gibbs free energy of mixing (ΔG_{mix}), power density (PD), efficiency (η), percent of frictional / resistive losses, uncontrolled mixing losses, and unutilized energy, applied hydraulic pressure (ΔP), and area-specific load resistance ($R_L A_m$) for the scenarios investigated.

Seawater-River Water (0.6 M-1.5 mM NaCl)				
ΔG_{mix} (kWh/m^3)	0.56			
	PRO-I	PRO-II	RED-I	RED-II
PD (W/m^2)	2.39	3.69	0.767	1.05
Efficiency, η (%)	53.9	44.1	37.8	31.1
Frictional / resistive losses (%)	14.9	17.8	6.7	6.8
Uncontrolled mixing losses (%)	28.9	30.5	45.3	39.4
Unutilized energy (%)	2.2	7.6	10.2	22.7
ΔP (bar)	14.2	13.1		
$R_L A_m$ (Ωcm^2)			9.15	6.05
Brine-Wastewater (1.2 M-10 mM NaCl)				
ΔG_{mix} (kWh/m^3)	1.08			
	PRO-I	PRO-II	RED-I	RED-II
PD (W/m^2)	6.85	8.86	0.861	0.863
Efficiency, η (%)	53.9	45.7	33.1	22.6
Frictional / resistive losses (%)	16.5	18.2	7.0	7.0
Uncontrolled mixing losses (%)	28.3	30.8	36.3	28.7
Unutilized energy (%)	1.2	5.3	23.6	41.7
ΔP (bar)	28.6	26.3		
$R_L A_m$ (Ωcm^2)			7.63	6.25
Engineered Solutions (4.0 M-17 mM NaCl)				
ΔG_{mix} (kWh/m^3)	3.68			
	PRO-I	PRO-II	RED-I	RED-II
PD (W/m^2)	38.0	40.2	1.15	1.75
Efficiency, η (%)	56.1	47.8	18.1	5.5
Frictional / resistive losses (%)	15.0	16.9	8.3	11.6
Uncontrolled mixing losses (%)	28.1	31.0	19.2	6.1
Unutilized energy (%)	0.8	4.3	54.4	76.8
ΔP (bar)	96.7	88.9		
$R_L A_m$ (Ωcm^2)			6.82	4.19